International Tables for X-ray Crystallography (1974). Vol. IV. Kynoch Press. (Present distributors Kluwer Academic Publishers, Dordrecht.)
ISCC–NBS (INTER-SOCIETY COLOR COUNCIL–NATIONAL BUREAU OF STANDARDS) (1964). *Color-Name Charts*, supplement to NBS Circular 553. ISCC–NBS, Washington, DC.
JOHNSON, C. K. (1969). *Acta Cryst.* A**25**, 187–194.
KENNARD, O., SPEAKMAN, J. C. & DONNAY, J. D. H. (1967). *Acta Cryst.* **22**, 445–449.
LISSALDE, F., ABRAHAMS, S. C. & BERNSTEIN, J. L. (1978). *J. Appl. Cryst.* **11**, 31–34.
NAKAMURA, D., ITO, K. & KUBO, M. (1962). *J. Am. Chem. Soc.* **84**, 163–166.
POHL, S. & SAAK, W. (1985). *Z. Naturforsch. Teil B*, **40**, 251–257.
RÖSSLER, K. & WINTER, J. (1977). *Chem. Phys. Lett.* **46**, 566–570.
YOUNG, R. A., MACKIE, P. E. & VON DREELE, R. B. (1977). *J. Appl. Cryst.* **10**, 262–269.
ZUCKER, U. H. & SCHULZ, H. (1982). *Acta Cryst.* A**82**, 563–568.

Acta Cryst. (1989). B**45**, 34–40

Atomic Displacement, Anharmonic Thermal Vibration, Expansivity and Pyroelectric Coefficient Thermal Dependences in ZnO*

J. ALBERTSSON† AND S. C. ABRAHAMS
AT&T Bell Laboratories, Murray Hill, NJ 07974, *USA*
AND Å. KVICK
Chemistry Department, Brookhaven National Laboratory, Upton, NY 11973, *USA*

(*Received* 25 *April* 1988; *accepted* 11 *August* 1988)

Abstract

The thermal expansivity in zinc oxide, space group $P6_3mc$, has been remeasured dilatometrically in the range 298–900 K and normalized to the lattice constants measured at 298 K in a Bond lattice-constant diffractometer. The lattice constants have also been determined at 20 K in a four-circle diffractometer. The linear thermal-expansion coefficients are $\alpha_1^T = 6{\cdot}511 \times 10^{-6}[1 + 0{\cdot}693\,(20) \times 10^{-3}\Delta T - 0{\cdot}230\,(6) \times 10^{-6}(\Delta T)^2]\ K^{-1}$ and $\alpha_3^T = 3{\cdot}017 \times 10^{-6}[1 + 2{\cdot}56\,(7) \times 10^{-3}\Delta T - 3{\cdot}37\,(9) \times 10^{-6}(\Delta T)^2]\ K^{-1}$, where $\Delta T = T - 298$ K. The structure has been determined at 20, 300, 600 and 900 K by neutron diffraction, based respectively upon 584, 301, 364 and 364 symmetry independent averaged F_m^2. Evidence for thermal atomic vibration anharmonicity was present at 600 and 900 K, but was not detectable at 20 and 300 K. Appreciable extinction was found at all temperatures. The ionic displacement thermal-dependence coefficient is $0{\cdot}263\,(8) \times 10^{-4}$ Å K^{-1} between 20 and 900 K. The pyroelectric coefficients derived from a point-charge model, with point charge of $0{\cdot}21\,(5)e$ and nuclear positions corresponding to final $R = 0{\cdot}0225$, 0·0231, 0·0177 and 0·0182 at 20, 300, 600 and 900 K respectively, are +1(2), −11(4) and −11(5) × 10^{-6} C m^{-2} K^{-1} at 160, 450 and 750 K respectively compared with experimental values of −6, −10·3 and $-11{\cdot}6 \times 10^{-6}$ C m^{-2} K^{-1}.

* Part of this work was performed at the Brookhaven National Laboratory under contract DE-AC02-76CH00016 with the US Department of Energy and supported by its Division of Chemical Sciences, Office of Basic Energy Sciences. The work was also supported in part by the Swedish Natural Science Council.

† Permanent address: Inorganic Chemistry 2, Chemical Center, University of Lund, POB 124, S-22100 Lund, Sweden.

0108-7681/89/010034-07$03.00

Introduction

The microscopic origin of pyroelectricity in polar crystals has long been a topic of considerable interest. A direct relationship between atomic displacement and polarization temperature dependence has been developed in recent years for several pyroelectric crystals, see reviews by Abrahams (1978, 1979, 1985). Typical values of the pyroelectric coefficient range from 300 × 10^{-6} C m^{-2} K^{-1} for $BaMnF_4$ to $-3{\cdot}9 \times 10^{-6}$ C m^{-2} K^{-1} for $LiClO_4.3H_2O$, with larger values being generally associated with ferroelectric crystals. These coefficients have been used to derive the corresponding ionic displacement temperature coefficients; that for $BaMnF_4$ is $0{\cdot}9 \times 10^{-3}$ Å K^{-1} and for $LiClO_4.3H_2O$ is $0{\cdot}03 \times 10^{-3}$ Å K^{-1}, for example. Among the first pyroelectric crystals for which the ionic displacement temperature coefficient was measured experimentally in relation to the pyroelectric coefficient was $Ba(NO_2)_2.H_2O$ (Liminga, Abrahams, Glass & Kvick, 1982); with a value for the compound of $0{\cdot}44\,(1) \times 10^{-3}$ Å K^{-1}, a polarization change of $-3{\cdot}0 \times 10^{-3}$ C m^{-2} was calculated between 102 and 298 K compared with a measured value of $-2{\cdot}6 \times 10^{-3}$ C m^{-2}. Similarly, the polarization change in $Li_2SO_4.H_2O$ between 80 and 298 K was calculated from the nuclear positions as $-11{\cdot}8 \times 10^{-3}$ C m^{-2} (Karppinen, Liminga, Kvick & Abrahams, 1988),

whereas the experimental value is $10{\cdot}4 \times 10^{-3}$ C m^{-2} (the absolute sign was not determined in the macroscopic measurement). Unambiguous derivation of the polarization change, from the ionic position thermal dependence, was not possible in the study of α-$LiIO_3$ (Svensson, Albertsson, Liminga, Kvick & Abrahams, 1983) despite an extensive diffraction investigation.

Temperature-dependent relative ionic displacements necessarily result in modified charge distributions as the Coulombic forces between the ions change. The electric multipole components associated with a system of variable charges must also be temperature dependent in pyroelectric crystals (Buckingham, 1959). The resulting complexity in polyatomic systems, such as those previously investigated, is considerably reduced by studying a diatomic system. A pyroelectric diatomic material that has already been intensively studied is ZnO, which crystallizes with the wurzite structure.

The pyroelectric coefficient for ZnO was first reported by Bateman (1962) and by Heiland & Ibach (1966) as about $-9{\cdot}4 \times 10^{-6}$ C m^{-2} K^{-1}. The valence pseudocharge density in ZnO was calculated for a single temperature, by Chelikowsky (1977). A rigid-ion model was used by Grout, March & Lewis (1981) to show that the pyroelectric coefficient of ZnO is proportional to the mean-square displacement of the ions over a wide temperature range, with the displacements given by an anharmonic oscillator. Kihara & Donnay (1985), hereafter KD, reported a structural refinement of ZnO at 293 and 473 K in which the thermal motion of the two atoms is modelled by inclusion of second- and third-order cumulant-expansion terms. In order to achieve structural refinement, KD set the $\gamma(111)$ term for O identical to that of Zn whereas $\gamma(113)$ and $\gamma(333)$ for O were set equal to but with opposite sign from that of the corresponding term for Zn. Donnay (1985) found that her $\gamma(111)$ term gave a secondary pyroelectric coefficient of value -10×10^{-6} C m^{-2} K^{-1} whereas an experimental value of $-2{\cdot}5 \times 10^{-6}$ C m^{-2} K^{-1} has been reported (Bateman, 1962). However, the total pyroelectric coefficient given by her structural parameters based on an anharmonic thermal-motion refinement was -48×10^{-6} C m^{-2} K^{-1} whereas that obtained from the harmonic thermal motion refinement is $+1{\cdot}5 \times 10^{-6}$ C m^{-2} K^{-1}.

In view of the rather poor fit given both by the previous harmonic and the anharmonic thermal-vibration models, and our interest in studying a simple diatomic pyroelectric system, we undertook a neutron diffraction investigation of ZnO at 20, 300, 600 and 900 K, and present the results below.

Experimental

The crystal used in this study was cut from a larger crystal grown hydrothermally by Airtron Litton Industries (Laudise, Kolb & Caporaso, 1964). The crystal was bounded by $\pm(10.0)$, $\pm(1\bar{2}.0)$ and $\{00.1\}$ with dimensions $2{\cdot}35 \times 2{\cdot}35 \times 2{\cdot}53$ mm, for a volume of $14{\cdot}0$ mm^3. It was mounted on an aluminium pin attached to the cold finger of an Air Products and Chemicals Inc. Model CS-202 Displex® closed-cycle refrigerator within a helium-filled aluminium can. A platinum resistance thermometer was used to monitor the crystal temperature, which was maintained at 20 ± 1 K. The measurements at 300, 600 and 900 K were carried out in the furnace built by Abrahams, Buehler, Hamilton & LaPlaca (1973), with a rebuilt but basically similar control system. The two higher temperatures did not vary more than ± 2 K. All neutron diffraction measurements were performed at the Brookhaven National Laboratory High Flux Beam Reactor.

Table 1. *Experimental and crystal data for* ZnO

Measurement temperature (K)	20, 300, 600, 900
No. of reflections for cell parameters	32, 29, 30, 30
Range in 2θ (°)	46–57
D_m (g cm^{-3})*	5·642(12) at 300 K
D_x (g cm^{-3})	5·674 at 300 K
λ (Å)†	0·81584, 0·833, 0·833, 0·833
Monochromator	Ge(331)
μ (mm^{-1})	0·0025
Transmission-factor range (%)	0·9940–0·9949
Reciprocal lattice point scan (°)	$\Delta 2\theta = -1{\cdot}99\ (1-4{\cdot}86 \tan\theta)$ for $2\theta \geq 60°$, $\Delta 2\theta = 3°$ for $2\theta \leq 60°$
Reciprocal lattice point range	$-4 \leq h \leq 4, 0 \leq k \leq 6, -10 \leq l \leq 10$
Max. $(\sin\theta)/\lambda$ (Å^{-1})	0·988, 0·967, 0·967, 0·966
Time per reciprocal lattice point (s)	120–180
Total No. of F_m^2	1160, 394, 470, 631
No. of independent $\langle F_m^2 \rangle \geq 3\sigma(F_m^2)$	584, 301, 364, 364
No. of standard reflections	2
Standard reflection measurement interval (h)	~3
R_{int}	0·036, 0·020, 0·009, 0·022
wR_{int}	0·050, 0·021, 0·011, 0·019

* Abrahams & Bernstein (1969).

† Wavelength calibrated using a standard KBr crystal [$a_0 = 6{\cdot}6000(1)$ Å] at 300 K.

The first set of integrated intensity measurements was made at 300 K and, on completion and reduction to structure factors, was immediately noted to be strongly affected by extinction as was also evidenced by recorded ψ scans. The next set of measurements was hence made at 900 K. A reduction in extinction was expected as a result of the thermal strain thereby imposed. The 600 K set was measured next, followed by a repeat of the 300 K set. Finally, the integrated intensities were measured at 20 K. The cooling rate throughout was 2 K min^{-1}.

The integrated intensities were determined by the method indicated in Table 1. The intensities of the standard reflections did not vary systematically during the course of the experiment. The integrated intensities were obtained by correcting each cumulative count for background, taken as the first and last 10% of the total scan. Corrections were made for Lorentz and absorption effects. Thermal diffuse-scattering effects calculated according to Stevens (1974) were found to be so small that correction was unnecessary.

Thermal expansivity of zinc oxide

Numerous values for the thermal linear expansion of ZnO have been reported [see Touloukian, Kirby, Taylor & Lee (1977) for a compilation and discussion]. Most reports agree that the expansivity of both axes is nonlinear, but give values that differ substantially at temperatures in the range 20–900 K. Thus, the recommended compilation values of Touloukian *et al.* (1977) at 300 K are $\alpha_1 = 5{\cdot}15 \times 10^{-6}\,K^{-1}$ and $\alpha_3 = 3{\cdot}05 \times 10^{-6}\,K^{-1}$ whereas the dilatometric values reported for example by O'Bryan, Van Uitert, Kolb & Zydik (1978) are $\alpha_1 = 6{\cdot}51 \times 10^{-6}\,K^{-1}$ and $\alpha_3 = 3{\cdot}71 \times 10^{-6}\,K^{-1}$ at 300 K. Accurate values for the lattice constants at each temperature studied in the present investigation are essential in deriving the total pyroelectric coefficient, hence the lattice constant of each axis was remeasured at room temperature and the thermal expansivity of both was redetermined over the range 298–900 K.

The Bond (1960) precision lattice-constant diffractometer was used to measure the spacings of the 00.6 and 30.0 reflections from a plate taken from the same crystal as used in the structure determinations. Barns' (1967) modification of Bond's method was employed, with the use of Cu $K\alpha_1$ radiation ($\lambda = 1{\cdot}540598$ Å, Deslattes & Henins, 1973). The procedure outlined by Abrahams, Liminga, Marsh, Schrey, Albertsson, Svensson & Kvick (1983) was adopted. Following correction to the standard temperature of 300 K, the resulting lattice constants are $a = 3{\cdot}249921\ (52)$ and $c = 5{\cdot}206578\ (83)$ Å. Previous values obtained by the same method (see Abrahams & Bernstein, 1969), and corrected to 300 K, are $a = 3{\cdot}249871\ (6)$ and $c = 5{\cdot}206625\ (2)$ Å. The increased standard deviations in the present measurements, as compared with the earlier values, are caused by the inclusion of both internal and external estimates of error. The differences between the two sets are not significant, and their average (in which the 1969 standard deviations are replaced by the more realistic present values) may be taken as the best lattice constants at 300 K, namely $a = 3{\cdot}249896\ (37)$ and $c = 5{\cdot}206602\ (59)$ Å.

The dilatometric measurements were made on samples cut from the same crystal as used for the Bond diffractometer. The crystal thickness along [10.0] was 4·24 mm, that along [00.1] was 5·00 mm. The method used was that given by Abrahams *et al.* (1983), for a heating rate of about 1 K min^{-1}. Values of $\Delta l/l_0$, where l_0 is the crystal thickness at 298 K and Δl is the dimensional change at the temperature T, were fitted by linear-regression analysis to the third-order polynomial:

$$\Delta l/l_0 = A_0 + A_1T + A_2T^2 + A_3T^3,$$

in which $A_0 = -0{\cdot}221663 \times 10^{-3}$, $A_1 = 6{\cdot}3966 \times 10^{-6}$, $A_2 = 2{\cdot}3148 \times 10^{-9}$ and $A_3 = -0{\cdot}484 \times 10^{-12}$ for the a axis and $A_0 = -0{\cdot}112522 \times 10^{-3}$, $A_1 = 2{\cdot}8172 \times 10^{-6}$, $A_2 = 4{\cdot}1287 \times 10^{-9}$ and $A_3 = -3{\cdot}378 \times 10^{-12}$ for the c axis.

Table 2. *Lattice constants and principal linear thermal-expansion coefficients in ZnO*

For $\alpha_i^T = \alpha_i^{298}[1 + C(1)_i\Delta T + C(2)_i(\Delta T)^2]$, see text. All coefficients are estimated to have a standard deviation of about 1%.

T (K)	α_1 (a axis) (10^{-6} K^{-1})	a axis (Å)	α_3 (c axis) (10^{-6} K^{-1})	c axis (Å)
20	–	3·2417 (8)*	—	5·1876 (8)*
300	6·51	3·24992 (5)	3·02	5·20658 (8)
400	6·96	3·25210 (5)	3·70	5·20830 (8)
500	7·36	3·25439 (5)	4·17	5·21030 (8)
600	7·74	3·25682 (5)	4·43	5·21251 (8)
700	8·08	3·25937 (5)	4·49	5·21483 (8)
800	8·40	3·26203 (5)	4·34	5·21716 (8)
900	8·69	3·26480 (5)	3·99	5·21939 (8)

* Derived from the four-circle neutron diffractometer measurements, see Table 1.

Recasting (Abrahams *et al.*, 1983) to the more convenient form used by Touloukian *et al.* (1977):

$$\alpha_i^T = \alpha_i^{298}[1 + C(1)_i\Delta T + C(2)_i(\Delta T)^2]$$

where α_i^T is the linear thermal-expansion coefficient at the temperature T along the ith axis, $\Delta T = T - 298$ K, $\alpha_1^{298} = 6{\cdot}511 \times 10^{-6}$ and $\alpha_3^{298} = 3{\cdot}017 \times 10^{-6}$ K^{-1}, then $C(1)_1 = 0{\cdot}693\ (20) \times 10^{-3}$, $C(2)_1 = -0{\cdot}230\ (6) \times 10^{-6}$, $C(1)_3 = 2{\cdot}56\ (7) \times 10^{-3}$ and $C(2)_3 = -3{\cdot}37\ (9) \times 10^{-6}$. The values presented in Table 2 are thereby obtained.

The lattice constants recently reported by KD may be corrected from their measurement temperatures of 293 and 473 K to give $a_{300} = 3{\cdot}2494$, $a_{500} = 3{\cdot}2535$, $c_{300} = 5{\cdot}2038$ and $c_{500} = 5{\cdot}2074$ Å. Comparison with the lattice constants in Table 2 shows all four values to be systematically low, but with differences that are not statistically significant in terms of their e.s.d.'s. Corresponding values of $\alpha_1 = 6{\cdot}4$, $\alpha_3 = 4{\cdot}3 \times 10^{-6}$ K^{-1} at 293 K were reported by KD.

Structural refinement

The method of least squares was used to refine the structure of ZnO in space group $P6_3mc$ at 20, 300, 600 and 900 K based on the structure amplitudes measured as outlined in Table 1.* The quantity minimized was $\sum w(|F_m| - |F_c|)^2$, where the weight w is given by the arbitrary relationship $w = [\sigma^2_{c.s.}(|F_m|) + (a|F_m|)^2 + b]^{-1}$ and $a = 0{\cdot}025$, 0·030, 0·020 and 0·020 for the 20, 300, 600 and 900 K data respectively, and b is zero except for the data at 20 K for which it is 0·0005. The initial

* Lists of structure factors measured at 20, 300, 600 and 900 K (including F_c, σF_m and the extinction correction) and anharmonic thermal parameters at 600 and 900 K have been deposited with the British Library Document Supply Centre as Supplementary Publication No. SUP 51233 (38 pp.). Copies may be obtained through The Executive Secretary, International Union of Crystallography, 5 Abbey Square, Chester CH1 2HU, England.

Table 3. *Mosaic spread and maximum extinction correction in* ZnO *at* 20, 300, 600 *and* 900 K

Temp. (K)	Mosaic spreads (s) 1	2	3	Max. correction hkl	Corr.
20	8·96	6·35	3·14	$\bar{1}10$	1·91
300	11·1	7·11	1·06	002	2·26
600	19·4	6·18	5·24	$\bar{1}20$	1·73
900	19·5	5·47	4·98	$\bar{1}20$	1·70

model placed Zn at $\frac{1}{3},\frac{2}{3},0$ and O at $\frac{1}{3},\frac{2}{3},z$ with $z = 0{\cdot}3825$ (Abrahams & Bernstein, 1969). The program used was *UPALS* (Lundgren, 1982), run on our VAX computers. The scattering lengths were taken as $b(\mathrm{Zn}) = 5{\cdot}680$, $b(\mathrm{O}) = 5{\cdot}805$ fm (Commission on Neutron Diffraction, 1982).

The initial set of structure amplitudes measured at 300 K was found to be strongly affected by extinction (see *Experimental*), hence these data were not used in refinement but were replaced by the set measured after the 900 and 600 K sets. The remaining extinction in the hydrothermally grown crystal was found to be markedly anisotropic, as determined by including the Becker & Coppens (1974, 1975) formalism in the least-squares refinement, assuming a Lorentzian angular mosaic distribution (Thornley & Nelmes, 1974). The resulting mosaic spread along the three principal ellipsoid axes at each temperature is given in Table 3, together with the corresponding maximum correction on F_m. Structure factors with corrections greater than 1·50 were given zero weight before the final cycles of least-squares refinement were undertaken. A total of 7, 14, 3 and 4 structure factors measured respectively at 20, 300, 600 and 900 K were hence eliminated from least-squares minimization (see deposition footnote).

Anisotropy was present in the thermal vibrations of both atoms at all temperatures and a minor anharmonic component was detectable in the structure amplitudes measured at 600 and 900 K. For these two sets, the third-order tensor coefficients were included in the Gram–Charlier expansion of the probability density function within the *UPALS* program. The hypothesis that thermal motion in ZnO at 600 and 900 K should be described by a harmonic rather than an anharmonic model may be rejected at the 99·5% confidence level on the basis of Hamilton's (1965) $\mathcal{R}$ test. The ratio of wR for the two models is 1·063 at 600 K and 1·173 at 900 K, whereas $\mathcal{R}_{6,346,0.005} = 1{\cdot}028$. Refinement of fourth- and fifth-order coefficients gave no further improvement in wR. The final values of the resulting z coordinate for O at each temperature investigated and the corresponding anisotropic thermal parameters are given in Table 4. The final refinement indicators are presented in Table 5. The generally linear δR plots with small intercepts (Table 5) show that the deviates $\delta R = (|F_m| - |F_c|)/\sigma F_m$ (where $\sigma F_m = w^{-1/2}$) are randomly distributed and hence that both measurement and model are most likely free from bias. Fig. 1 shows the Zn–O tetrahedra in ZnO at 20, 300, 600 and 900 K, illustrating the thermal ellipsoids at the 95% probability level.

Table 4. *Positional coordinate and anisotropic temperature coefficients in* ZnO *at* 20, 300, 600 *and* 900 K

The form of the anisotropic thermal factor is $\exp[-2\pi^2(U_{11}a^{*2}h^2 + U_{22}b^{*2}k^2 + U_{33}c^{*2}l^2 + 2U_{12}a^*b^*hk + 2U_{23}b^*c^*kl + 2U_{31}c^*a^*lh)]$.

Temp. (K)	z (O)	U_{11} (Zn) (Å²)	U_{33} (Zn) (Å²)	U_{11} (O) (Å²)	U_{33} (O) (Å²)
20	0·3819 (1)	0·0009 (1)	0·0003 (1)	0·0025 (2)	0·0045 (2)
300	0·3819 (1)	0·0073 (4)	0·0094 (4)	0·0056 (4)	0·0064 (4)
600	0·3829 (3)	0·0115 (3)	0·0117 (6)	0·0144 (4)	0·0168 (7)
900	0·3841 (3)	0·0167 (3)	0·0184 (5)	0·0209 (4)	0·0226 (7)

Table 5. *Refinement indicators of agreement*

Temp. (K)	$R(F)$	$wR(F)$	S	m	$\mathscr{S}$*	t*
20	0·0225	0·0286	0·705	12	0·79	0·06
300	0·0231	0·0367	1·126	12	1·02	0·04
600	0·0177	0·0238	0·971	15	0·94	0·00
900	0·0182	0·0220	0·864	15	0·85	0·06

* From the δR plot (Abrahams & Keve, 1971).

Temperature dependence of atomic positions

The location of the O atoms (on the trigonal axes) with respect to the Zn atoms appears to remain unchanged within the unit cell between 20 and 300 K but becomes increasingly temperature dependent above 300 K, see Table 4. In combination with the thermal expansivity of the unit cell, see Table 2, the thermal dependence of the atomic positions results in the apical (along the c axis) and basal (inclined at about 108° to the c axis) bond lengths and angles given in Table 6.

It is notable that both bond lengths exhibit a highly significant temperature dependence, whereas the bond angles are more nearly independent of temperature, within the calculated e.s.d.'s. The present values at

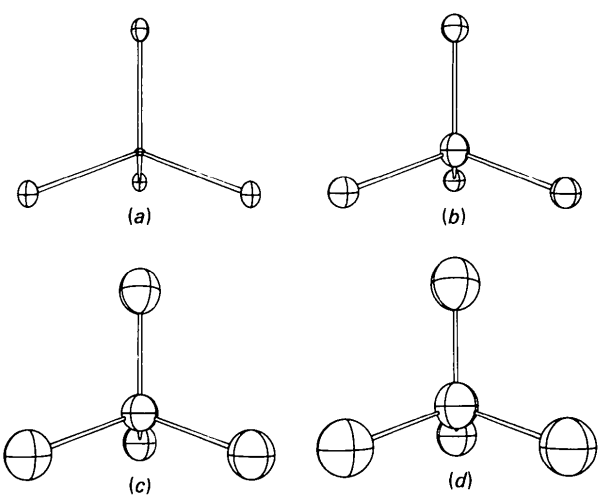

Fig. 1. Zn–O tetrahedra in ZnO at (*a*) 20, (*b*) 300, (*c*) 600 and (*d*) 900 K with thermal ellipsoids drawn at the 95% probability level.

Table 6. *Bond lengths and angles in* ZnO *at* 20, 300, 600 *and* 900 K

Temp. (K)	Bond length Apical (Å)	Bond length Basal (Å)	Bond angle Apical (°)	Bond angle Basal (°)
20	1·9815 (7)	1·9692 (5)	108·11 (2)	110·79 (2)
300	1·9882 (6)	1·9746 (2)	108·15 (2)	110·76 (2)
600	1·9961 (16)	1·9768 (5)	107·98 (4)	110·92 (4)
900	2·0047 (14)	1·9796 (4)	107·79 (4)	111·10 (4)

300 K are not significantly different from those reported by KD at 293 K.

It may also be seen from Table 6 that the thermal dependence of the ionic displacement between 20 and 900 K is 0·263 (8) $\times 10^{-4}$ Å K^{-1}. This coefficient is at the lower end of the range given by Abrahams (1985), although it is closely comparable with that in $LiClO_4 \cdot 3H_2O$ (Abrahams, 1978).

Fig. 2 presents the probability density functions at 600 and 900 K, mapped on a plane containing the apical and one basal Zn—O bond. The primary directions of anharmonic thermal motion appear to rotate 180° between the two temperatures. The physical significance of this result may, however, be small since the values of the tensor coefficients are not highly significant.

Debye temperature

The weighted mean-squared radial amplitudes of atomic vibration at three measurement temperatures, derived from the anisotropic temperature coefficients in Table 4, are 0·0076 (2), 0·0123 (2) and 0·0181 (2) $Å^2$ at 300, 600 and 900 K respectively. The corresponding Debye temperatures, for an average atomic mass of 40·69 and neglecting the anharmonic vibration component, are 384 (5), 420 (3) and 423 (3) K respectively. The Debye temperature may also be estimated from the room-temperature elastic constants (Tokarev, Karyakina, Kobyakov, Kuz'mina & Lobachev, 1973). The resulting mean sound velocity, calculated according to Robie & Edwards (1966), is $v_s = 3230$ m s^{-1} leading to a Debye temperature of $\Theta_D = 421$ K. Previous values for Θ_D, based on diffraction analysis, are 370 K (Abrahams & Bernstein, 1969) and 387 K at room temperature and 393 K at a temperature of 473 K (KD).

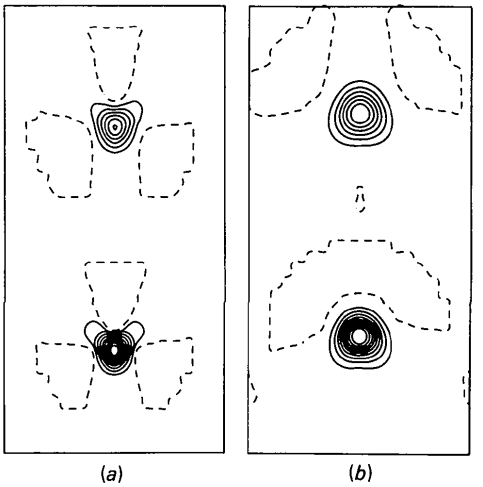

Fig. 2. Probability density maps of Zn and O at (*a*) 600 and (*b*) 900 K. The lower atom is Zn. The maps were computed with the *PDF*187 program and drawn on an arbitrary scale by the *CONTOUR* program (Craven & Weber, 1987).

Primary and secondary pyroelectricity

The total pyroelectric coefficient p_3 for ZnO has been reported in the range 9–425 K by Heiland & Ibach (1966) and has specific values $-0{\cdot}28 \times 10^{-6}$ C m^{-2} K^{-1} at 20 K and $-9{\cdot}4 \times 10^{-6}$ C m^{-2} K^{-1} at 300 K, with extrapolated values of -11×10^{-6} C m^{-2} K^{-1} at 600 K and -12×10^{-6} C m^{-2} K^{-1} at 900 K. The coefficient p_3 is the sum of the primary coefficient p_3' and the secondary coefficient p_3'', where p_3' is a measure of the polarization that would be produced by a temperature change in which the shape and volume of the crystal are constant, *i.e.* p_3' is due entirely to the relative thermally dependent displacements of the ions in the unit cell, and p_3'' is a measure of the polarization caused only by thermal expansion of the crystal lattice [see, for example, Nye (1957)].

The secondary contribution to the pyroelectric effect in ZnO may be calculated as $p_3'' = 2e_{31}\alpha_1 + e_{33}\alpha_3$, where e_{ij} are piezoelectric stress coefficients and α_j are thermal-expansion coefficients. Taking $e_{31} = -0{\cdot}62$ and $e_{33} = 0{\cdot}96$ C m^{-2} from Tokarev, Kobyakov, Kuz'mina, Lobachev & Pado (1975) and α_j^{300} from Table 2 gives $p_3'' = -5{\cdot}2 \times 10^{-6}$ C m^{-2} K^{-1}. The resulting primary pyroelectric coefficient at 300 K is hence $-4{\cdot}2 \times 10^{-6}$ C m^{-2} K^{-1}. It may be noted that the ratio p_j'/p_j'' varies widely with material, but is generally within a range on the order of 10^2 to 10^{-2} (Abrahams, 1980).

Piezoelectric contribution to thermal expansivity

The thermal expansivity of ZnO may be treated analogously with its pyroelectricity, see the preceding section. The pyroelectric polarization resulting from a change in temperature necessarily causes a piezoelectric deformation of the crystal lattice as given by $\alpha_i^D = \alpha_i^E - d_{3i}\beta_3 p_3$, see Nye (1957), where the superscript D denotes constant displacement or electrically clamped and E denotes constant field or electrically free, the d_{3i}'s are piezoelectric strain coefficients, and $\beta_3 = 1/\varepsilon_0 K_3$ ($\varepsilon_0 = 8{\cdot}85$ pF m^{-1} is the permittivity of a vacuum and K_3 is the relative permittivity at constant stress along the polar direction). Taking the room-temperature values for ZnO as $d_{31} = -5{\cdot}12$, $d_{33} = 12{\cdot}3$ pC N^{-1} and $K_3 = 11{\cdot}26$ (Tokarev *et al.*, 1975), then $\alpha_1^D = 6{\cdot}04 \times 10^{-6}$ and $\alpha_3^D = 4{\cdot}16 \times 10^{-6}$ K^{-1}.

Comparison with the electrically free thermal-expansion coefficients at 300 K given in Table 2 shows that the piezoelectric lattice deformation in ZnO is about 7% of the measured thermal expansivity along the α axis and about 38% in the opposite sense along the polar direction.

Pyroelectric coefficient thermal dependence

A point-charge model may be used together with the structural results obtained above to estimate the total polarization P, on the assumption that the zinc and oxide ions carry equal but opposite point charges q that remain invariant with temperature and that there is negligible electronic redistribution with temperature. Considering the distorted tetrahedron of oxide ions about Zn (Fig. 1), the apical O located zc from Zn produces a negative dipole zcq; the three basal O ions each similarly produce a positive dipole of magnitude $3(\frac{1}{2}-z)cq$. The net polarization along the positive c axis is hence:

$$P = -2[z - 3(\tfrac{1}{2} - z)]cq/V = -(16z - 6)q/(3)^{1/2}a^2,$$

since each unit cell of volume V contains two ZnO. The resulting polarizations are $-6{\cdot}08\,(11) \times 10^{17}q\ \mathrm{m}^{-2}$ at 20 K, $-6{\cdot}00\,(10) \times 10^{17}q\ \mathrm{m}^{-2}$ at 300 K, $-6{\cdot}91\,(23) \times 10^{17}q\ \mathrm{m}^{-2}$ at 600 K and $-7{\cdot}89\,(23) \times 10^{17}q\ \mathrm{m}^{-2}$ at 900 K.

Experimentally, the pyroelectric coefficient p_3 (= $\Delta P/\Delta T$) is reported to be close to zero at 20 K, rising rapidly thereafter to about 350 K and then increasing only slightly more rapidly than linearly (Heiland & Ibach, 1966). The corresponding polarization is thus close to constant at very low temperatures, rising sharply from about 20 K until the rate of increase is only slightly greater than linear above 350 K.

The point-charge calculation gives a rather linear polarization thermal dependence between 300 and 900 K (see Fig. 3) with average $\Delta P/\Delta T = -3{\cdot}1\,(6) \times 10^{14}q\ \mathrm{m}^{-2}\,\mathrm{K}^{-1}$; between 20 and 300 K the calculated polarization is rather constant, with corresponding $\Delta P/\Delta T \sim 0$. The mean experimental value of $\Delta P/\Delta T$ between 300 and 500 K is $-10{\cdot}2 \times 10^{-6}\ \mathrm{C\ m^{-2}\,K^{-1}}$. With the elementary charge e taken as $1{\cdot}602 \times 10^{-19}$ C, then $q \simeq 0{\cdot}21\,(5)e$. Experimental and calculated values for p_3 at 160, 450 and 750 K (taken midway between the diffraction measurement temperatures) are hence -6 and $+1(2)$; $-10{\cdot}3$ and $-11(4)$; $-11{\cdot}6$ and $-11(5) \times 10^{-6}\ \mathrm{C\ m^{-2}\,K^{-1}}$.

A pyroelectric model based on the present structural results, in which the two kinds of ion are assigned point charges of $0{\cdot}21e$, hence gives a pyroelectric coefficient magnitude in general agreement with experiment at $T \geq 300$ K. An alternative estimate of the ionic point charge can be obtained by Phillips' (1973) energy-gap approach, in which $q = ef_i/2$, $E_g = E_h + iC$ and $f_i = C^2/E_g^2$ (where E_h and C are bond parameters with values in ZnO of 7·33 and 9·30 eV, respectively). The resulting value of $q = 0{\cdot}31e$ is in fair agreement with our pyroelectric estimate.

The calculated magnitudes of p_3 above 300 K are in excellent agreement with experiment; however, the value calculated at low temperatures is of opposite sign. A possibly important missing component in the change of polarization is that due to electronic redistribution with temperature. It is expected that a measure of such redistribution may be obtained from a one-particle potential and multipolar analysis of the charge density determined from the X-ray scattering by a ZnO crystal and the present neutron results, and a corresponding study is now in progress.

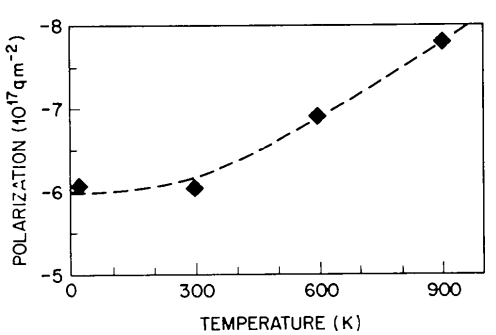

Fig. 3. Thermal dependence of the polarization in ZnO as calculated from the structure. The dashed line is only to guide the eye: the polarization dependence between 300 and 900 K is notably linear.

It is a pleasure to thank Dr Roger F. Belt for providing many samples of hydrothermally grown ZnO, P. Marsh for assistance with some of the neutron diffraction and the room-temperature lattice-constant measurements, Dr H. M. O'Bryan and Dr P. K. Gallagher for the dilatometric measurements, Professor B. M. Craven for providing a copy of the *PDF*187 program, and a referee for suggesting that we evaluate the secondary pyroelectric coefficient and the piezoelectric contribution to the thermal expansivity of ZnO.

References

ABRAHAMS, S. C. (1978). *Mater. Res. Bull.* **13**, 1253–1258.
ABRAHAMS, S. C. (1979). *God. Jugosl. Cent. Kristalogr.* **14**, 1–12.
ABRAHAMS, S. C. (1980). *Encyclopedia of Physics*, edited by R. G. LERNER & G. L. TRIGG, pp. 798–799. Reading: Addison–Wesley.
ABRAHAMS, S. C. (1985). *Aust. J. Phys.* **38**, 289–298.
ABRAHAMS, S. C. & BERNSTEIN, J. L. (1969). *Acta Cryst.* B**25**, 1233–1236.
ABRAHAMS, S. C., BUEHLER, E., HAMILTON, W. C. & LAPLACA, S. J. (1973). *J. Phys. Chem. Solids*, **34**, 521–532.
ABRAHAMS, S. C. & KEVE, E. T. (1971). *Acta Cryst.* A**27**, 157–165.
ABRAHAMS, S. C., LIMINGA, R., MARSH, P., SCHREY, F., ALBERTSSON, J., SVENSSON, C. & KVICK, Å. (1983). *J. Appl. Cryst.* **16**, 453–457.
BARNS, R. L. (1967). *Mater. Res. Bull.* **2**, 273–282.
BATEMAN, T. B. (1962). *J. Appl. Phys.* **33**, 3309 3312.

BECKER, P. & COPPENS, P. (1974). *Acta Cryst.* A**30**, 129–147; 148–153.
BECKER, P. & COPPENS, P. (1975). *Acta Cryst.* A**31**, 417–425.
BOND, W. L. (1960). *Acta Cryst.* **13**, 814–818.
BUCKINGHAM, A. D. (1959). *Q. Rev.* **13**, 183–214.
CHELIKOWSKY, J. R. (1977). *Solid State Commun.* **22**, 351–354.
COMMISSION ON NEUTRON DIFFRACTION (1982). December Newsletter.
CRAVEN, B. M. & WEBER, H. P. (1987). Private communication.
DESLATTES, R. D. & HENINS, A. (1973). *Phys. Rev. Lett.* **31**, 972–975.
DONNAY, G. (1985). *Can. Mineral.* **23**, 655–658.
GROUT, P. J., MARCH, N. H. & LEWIS, J. W. E. (1981). *Ferroelectrics*, **33**, 167–172.
HAMILTON, W. C. (1965). *Acta Cryst.* **18**, 502–510.
HEILAND, G. & IBACH, H. (1966). *Solid State Commun.* **4**, 353–356.
KARPPINEN, M., LIMINGA, R., KVICK, Å & ABRAHAMS, S. C. (1988). *J. Chem. Phys.* **88**, 351–355.
KIHARA, K. & DONNAY, G. (1985). *Can. Mineral.* **23**, 647–654.
LAUDISE, R. A., KOLB, E. D. & CAPORASO, A. J. (1964). *J. Am. Ceram. Soc.* **47**, 9–12.
LIMINGA, R., ABRAHAMS, S. C., GLASS, A. M. & KVICK, Å. (1982). *Phys. Rev. B*, **26**, 6896–6900.
LUNDGREN, J.-O. (1982). Report UUIC-B13-4-05. Institute of Chemistry, Univ. of Uppsala, Sweden.
NYE, J. F. (1957). *Physical Properties of Crystals*. Oxford Univ. Press.
O'BRYAN, H. M., VAN UITERT, L. G., KOLB, E. D. & ZYDIK, G. (1978). *J. Am. Ceram. Soc.* **61**, 269.
PHILLIPS, J. C. (1973). *Bonds and Bands in Semiconductors*. New York: Academic Press.
ROBIE, R. A. & EDWARDS, J. L. (1966). *J. Appl. Phys.* **37**, 2659–2663.
STEVENS, E. D. (1974). *Acta Cryst.* A**30**, 184–189.
SVENSSON, C., ALBERTSSON, J., LIMINGA, R., KVICK, Å. & ABRAHAMS, S. C. (1983). *J. Chem. Phys.* **78**, 7343–7352.
THORNLEY, F. R. & NELMES, R. J. (1974). *Acta Cryst.* A**30**, 748–757.
TOKAREV, E. F., KARYAKINA, N. F., KOBYAKOV, I. B., KUZ'MINA, I. P. & LOBACHEV, A. N. (1973). *Izv. Akad. Nauk SSSR Ser. Fiz.* **37**, 2401–2403.
TOKAREV, E. F., KOBYAKOV, I. B., KUZ'MINA, I. P., LOBACHEV, A. N. & PADO, G. S. (1975). *Fiz. Tverd. Tela (Leningrad)*, **17**, 980–986.
TOULOUKIAN, Y. S., KIRBY, R. K., TAYLOR, R. E. & LEE, T. Y. R. (1977). *Thermophysical Properties of Matter*, Vol. 13. *Thermal Expansion*. New York: IFI/Plenum.

Acta Cryst. (1989). B**45**, 40–45

Long-Period Tetragonal Lattice Formation by Solid-State Alloying at the Interfaces of Bi–Mn Double-Layer Thin Films

BY KENTAROH YOSHIDA, TAKASHI YAMADA AND YOSHIHISA TANIGUCHI

Department of Applied Physics, Faculty of Engineering, Kobe University, Rokkodai, Nada, Kobe 657, *Japan*

(*Received* 18 *April* 1988; *accepted* 19 *September* 1988)

Abstract

Thin Bi–Mn double-layer films, consisting of a Bi layer of 300 Å in thickness and an Mn layer of 200 Å prepared by successive vacuum deposition, were heated at 538 K for 100–200 h. Transmission electron micrographs show that a long-period tetragonal lattice forms at their interfaces, whose lattice constants were $a = 17{\cdot}26$, $c = 10{\cdot}21$ Å. Near to the tetragonal lattice grains, structures preliminary to lattice formation were observed. Their electron diffraction and high-resolution micrographs show that the formation process can be divided into two stages. In the first stage, Bi and Mn atoms combine to form polyatomic clusters 16 Å in diameter, which have a twelvefold symmetry axis normal to the (001) surface of the Bi crystals. In the second stage, these polyatomic clusters arrange themselves to build up the long-range tetragonal order.

Introduction

Thin films of ferromagnetic MnBi alloy phases have been investigated because of their magneto-optic applications (Williams, Sherwood, Foster & Kelley, 1957). Unger & Stolz (1971) and Chen (1971) deposited a Bi layer onto a cleaved surface of mica and then an Mn layer onto the Bi layer. They heated this composite double-layer film at around 573 K for a few days. The present authors also prepared alloy films by the same procedure, but their samples were kept very thin (about 500 Å in total thickness) and were deposited onto very thin carbon films to allow transmission electron microscope observations. After heating of these thin composite films at 538 K for 100–200 h, the micrographs showed that the alloying process is not so simple as had been presumed. In the previous investigations of Unger & Stolz (1971), Chen (1971) and others (Iwama, Mizutani & Humphrey, 1972; Honda & Kusuda, 1974), Mn atoms were considered simply to diffuse into the underlying Bi crystals to form the MnBi crystal lattices. In the present thin specimen heated at low temperature, however, a number of long-period crystal lattices were found to appear during heating (Yoshida, Yamada & Taniguchi, 1987). Results concerning one of them, a tetragonal lattice, and its related structure are reported here.

0108-7681/89/010040-06$03.00